

See discussions, stats, and author profiles for this publication at: <https://www.researchgate.net/publication/224050627>

Modification of a Styryl Dye Binding Mode with Calf Thymus DNA in Vesicular Medium: From Minor Groove to Intercalative

ARTICLE *in* THE JOURNAL OF PHYSICAL CHEMISTRY B · APRIL 2012

Impact Factor: 3.3 · DOI: 10.1021/jp301211m · Source: PubMed

CITATIONS

22

READS

74

2 AUTHORS, INCLUDING:



Anamika Manna

8 PUBLICATIONS 59 CITATIONS

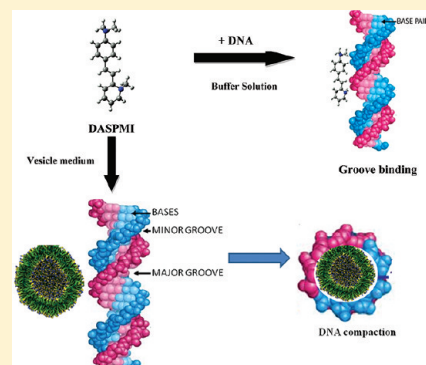
SEE PROFILE

Modification of a Styryl Dye Binding Mode with Calf Thymus DNA in Vesicular Medium: From Minor Groove to Intercalative

Anamika Manna and Sankar Chakravorti*

Department of Spectroscopy, Indian Association for the Cultivation of Science, Jadavpur, Kolkata 700032, India

ABSTRACT: This paper reports an interesting transformation of binding mode of 2-(4-(dimethylamino)styryl)-1-methylpyridinium iodide (DASPMI) with calf thymus DNA from minor groove binding in buffer solution to intercalative binding when the dye is encapsulated inside a vesicle formed by the interaction of 1,8-naphthalimide (a charge transfer dye) with the supramolecular association of sodium dodecyl sulfate and block-copolymer polyethylene-*b*-polyethylene glycol. The pre-encapsulated dye in the vesicular interior binds intercalatively to ct-DNA, as evinced by the high value of equilibrium binding constant of DASPMI–DNA complex, changes in CD-spectra of DNA and isosbestic point, along with downshift and hypochromicity of absorption band. Increase in anisotropy decay by 1.5 times with a single component strongly confirms restricted motion of the probe inside ct-DNA confirming intercalative binding. The compaction of ct-DNA caused by the interaction of the vesicle allows DASPMI to bind ct-DNA in the intercalative mode. However, the groove binding mode in ct-DNA–DASPMI remains unaffected by the retro-addition of the vesicles to the already bound dye to ct-DNA.



1. INTRODUCTION

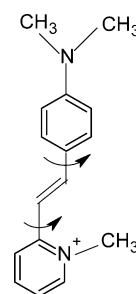
Binding studies of small molecules with deoxyribonucleic acid (DNA) are important in the design of new and more efficient drugs targeted to DNA^{1–3} and many chemical reagents of small molecular size have already proved to be useful as sensitive probes of local nucleic acid structure. Fluorophores that show an increase in fluorescence intensity on binding with the host act as useful markers in genomics and proteomics⁴ and are also widely used in microdetermination of the nucleic acids.^{5–9} These interactions of different small molecules with DNA provide relevant information for the development of the effective therapeutic agents in controlling gene expression.¹⁰ Various structural and electronic factors control the DNA binding affinity and sequence specificity of these small molecules.^{11,12} These different binding studies have widely been used in designing different useful anticancer agents for clinical use.¹ The discovery and development of novel therapeutic intercalative agents for the treatment of malignancy are some of the most important goals in modern medicinal chemistry. Drugs bind to DNA both covalently as well as noncovalently. Noncovalently bound drugs mostly fall under the following two classes: (1) minor groove binders and (2) intercalators. Covalent bonding is much stronger than noncovalent bonding. However, noncovalent binding is reversible and is typically preferred over covalent adducts. The noncovalent bonding intercalation is much stronger than groove binding. So, intercalators are mostly used in medicinal purposes.

Steric structures of the molecules generally determine the binding properties (such as binding affinity, binding mode) of the small molecules with the DNA. In general, the crescent structure of the molecules is an important feature for groove

binding and the planarity was suggested to be an important feature for intercalative binding.¹³

2-(4-(Dimethylamino)styryl)-1-methylpyridinium iodide (DASPMI) is an ionic styryl dye (Chart 1) which is known

Chart 1. Molecular Structure of DASPMI



to respond to changes in transmembrane potential by a fast electrostatic mechanism.^{14–16} The membrane potential of mitochondria^{17,18} in living cells is measured with this dye. Interesting multibond rotation due to the intramolecular charge transfer (ICT)^{2,19,20} is found to occur in DASPMI and the ICT state is highly sensitive to both polarity and microviscosity of the medium.²¹ In a previous paper we studied the interaction of DASPMI, with the ct-DNA²² in buffer solution and the fluorescence intensity of DASPMI was found to increase highly on interaction with ct-DNA. From different experimental and

Received: February 7, 2012

Revised: March 26, 2012

Published: April 16, 2012

theoretical docking it was confirmed that DASPMI forms complex with ct-DNA and the nature of binding was weak minor groove binding.

The block-copolymers self-assemble in aqueous solution to form spherical structures as studied theoretically by Srinivas et al. using coarse-grain dynamics.²³ In an earlier communication Sahoo et al. established²⁴ that the block-copolymer polyethylene-*b*-polyethylene glycol (PE-*b*-PEG) on interaction with an anionic surfactant sodium dodecyl sulfate (SDS) forms a water tight microenvironment due to the entanglement of the block-copolymer with the surfactant chains. Interestingly, interaction of a charge transfer dye 1,8 naphthalimide (NAPMD) (forms anion in aqueous solution by intermolecular charge transfer) with the above-mentioned block copolymer-micelle nanocomposite in aqueous solution gives some vesicle-like structures.²⁵ In another communication²⁶ we have demonstrated the nanocaging of DASPMI by these vesicles and its pH sensitive release from the vesicle interior on the basis of varying fluorescence resonance energy transfer (FRET) between DASPMI and NAPMD sitting on the surface of vesicular wall. Normally vesicles are very similar to modern cellular membranes²⁷ so these vesicular systems were considered to be an interesting medium to study their effect on the DASPMI-DNA binding properties in it vis-à-vis that in aqueous medium.²² There has been some work on encapsulation of DNA in cationic diblock copolymer vesicles²⁸ and its subsequent release, which is very important considering the wide futuristic application of nanosized polymeric vesicles. In order to use the NAPMD induced micelle-diblock-copolymer vesicles as a possible nanocarrier for drug and biomaterials, we thought to investigate the different aspects of binding characteristics of DNA in these vesicular media in detail. In this paper the DASPMI-DNA binding properties are envisaged to study with the help of steady state and time-resolved emission spectroscopy, anisotropy decay and circular dichroic spectroscopy, and scanning and transmission emission microscopy. From there we would then move on to investigating the stability of binding²² of DASPMI with DNA in the vesicle medium.

2. EXPERIMENTAL SECTION

2.1. Materials and Method. DASPMI was received from Aldrich Chemical and purified by vacuum sublimation. Ct-DNA was purchased from Sigma-Aldrich and was used without further purification. Potassium iodide (KI) was obtained from SRL and was used as received. Millipore water was used throughout the experiment. All experiments were done at room temperature (300 K) and at pH 7.

In 25 mM SDS micellar solution the block-copolymer is added (1 mg/mL) which forms a spherical nanocomposite and then in this nanocomposite on addition of 0.05 mM of NAPMD gives rise to formation of vesicles as described in our previous work.²⁴

2.2. Preparation of DNA Solutions. ct-DNA stock solution was prepared by dissolving the solid material, normally at 0.3 mg mL⁻¹, in distilled water. Then, the solution was kept overnight at 4 °C. The resulting viscous (somewhat) solution was clear and particle-free. Appropriate dilutions of the stock solutions were used in all the experiments. The stock solution was stored at -20 °C. The purity of ct-DNA was verified by monitoring the ratio of absorbance at 260 nm to that at 280 nm, which was in the range 1.8–1.9. The concentration of ct-DNA was determined spectrophotometrically (ϵ is the molar absorptivity in aqueous solution), using $\epsilon = 13\,600\text{ M}^{-1}\text{ cm}^{-1}$

(at 258 nm).²⁹ The molar absorptivity was expressed in terms of the base pairs. It was observed that the complex DASPMI-nucleic acid was induced by the concentration of Na⁺ ions. Due to this fact and the tendency of DASPMI to form complexes with the salts used in common buffer systems all spectroscopic measurements were performed in Millipore water with or without added sodium chloride. The pH of the sample solutions was adjusted by addition of small volumes of concentrated HCl or NaOH and was checked by using a digital meter.

2.3. Instruments. The absorption spectra at 300 K were recorded with a Shimadzu spectrophotometer (model UV-2104 PC) and emission spectra were obtained with a Hitachi F-4500 or Horiba Jobin Yvon Fluoromax 4 fluorescence spectrophotometer. The concentration of DASPMI used in all fluorescence experiments was about 0.05 mM, and emission was corrected for all of the optical components. Circular dichroism (CD) spectra were recorded on Jasco Corporation J-815 spectrophotometer using a rectangular quartz cuvette of path length 1 cm. Spectra shown are averages of three successive scans recorded at a scan speed of 50 nm/min, from which the appropriate blanks have been subtracted and the data were subjected to the noise reduction analysis. All of the experiments were performed at ambient temperature (300 K) with air equilibrated solutions. Throughout the experiment, the pH of the medium was kept constant at 7. The fluorescence picosecond lifetime measurement was done with a Horiba Jobin Yvon Fluoro Cube 01-NL time-resolved fluorescence lifetime spectrometer with the TBX-04 detector, Data Station measurement software, and DSA6 Foundation Package, and the excitation was done at 440 nm (diode laser). The instrument response function is ~80 ps.

Field emission scanning electron microscopy (FESEM; JSM-6700F, from JEOL, Japan) was used to record the scanning electron micrograph images of vesicle containing DASPMI and its interaction with ct-DNA in aqueous solution. A transmission electron microscope (JEOL, JEM-2010, Japan) operated at 2000 V, was employed for taking the TEM pictures.

3. RESULTS AND DISCUSSION

3.1. Absorbance Titration Results. The absorption studies were performed for DASPMI (0.05 mM) with addition of a certain concentration of the vesicle and varying the concentration of ct-DNA (Figure.1). The spectra for free DASPMI molecules show two bands at $\lambda_{ab} \approx 270\text{ nm}$ and $\sim 440\text{ nm}$. As depicted in our previous paper, the addition of ct-DNA to DASPMI quenches the 440 nm band with a slight red shift showing minor groove binding with the ct-DNA.²² In this study we observe that in presence of a certain concentration of vesicle the DASPMI 440 nm band (due to styryl moiety) shows hypochromism and the 270 nm band (due to phenyl moiety) shows hyperchromism with increasing concentration of ct-DNA along with an isosbestic point. Hypochromism is normally observed due to the strong interactions between the intercalating dye and that of the ct-DNA base pairs.³⁰ The absorption maximum at 440 nm also shows an extensive red shift to 452 nm probably due to the insertion of the dye into the nonpolar intercalation site of ct-DNA. The bathochromic shift of $\sim 12\text{ nm}$ is much greater than what we got in our previous study, i.e., $\sim 7\text{ nm}$.²² Thus the above spectral changes, i.e., hypochromism (at 440 nm), large red shift, and the presence of the isosbestic point, clearly give a hint that the styryl dye DASPMI binds strongly by intercalative binding to the ct-DNA base pairs in the presence of the vesicles.³¹ It is interesting to note that no change in the spectra of DASPMI could be

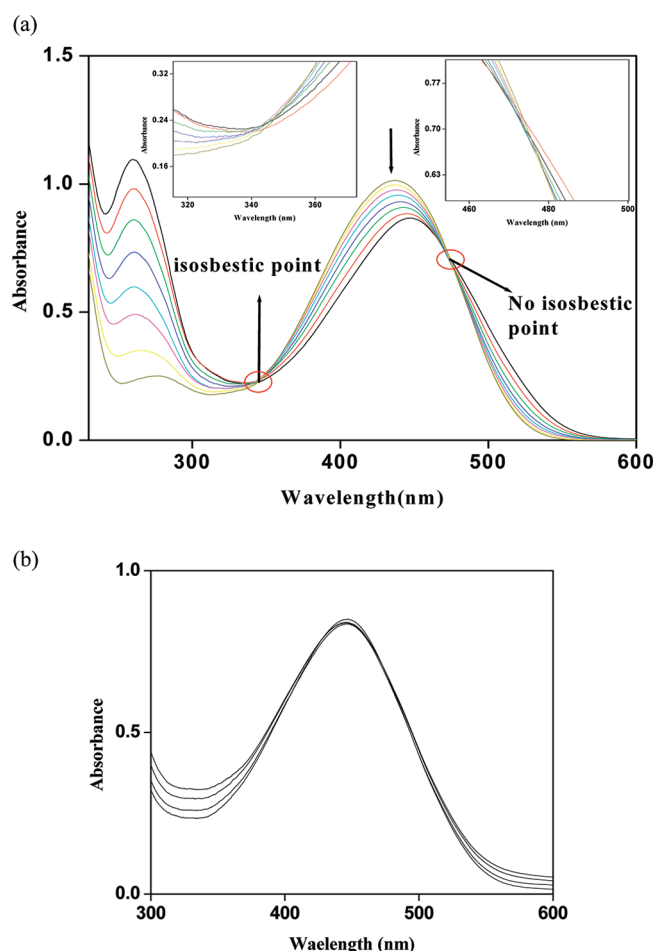


Figure 1. (a) Absorption spectra of DASPMI (0.05 mM) in vesicular medium with increasing concentration of ct-DNA. The arrows indicate how the absorbance of DASPMI responds to the increasing concentration of the DNA in the presence of the vesicles. ct-DNA concentration is increased as 0, 3, 6, 8, 12, 20, 40, and 60 μM . Inset: magnified images of the isosbestic and nonisosbestic points. (b) Absorption spectra of DASPMI for a certain concentration of ct-DNA, with gradual addition of vesicles to the already bounded DASPMI molecules with the ct-DNA.

observed even after long hours when the vesicles are gradually added to DASPMI molecules already bound to DNA (inset Figure 1). This observation shows that vesicles have no effect on the DASPMI molecules when bound to ct-DNA. To further understand the effect of the vesicles on the DASPMI bound with DNA we studied the absorbance of DASPMI with DNA in the block copolymer, with SDS and with NAPMD environments as well. None of them show any effect on the DASPMI binding mode with DNA.

The absorbance titration (Figure 2) results for the effect of vesicles on neat ct-DNA show that the absorption band of DNA at 260 nm gets quenched, broadened, and red-shifted by 3 nm. This possibly indicates a change in DNA structure. Interestingly the absorption of DNA remains almost unaffected by the vesicles when it is already bound to the DASPMI molecules.

3.2. Fluorescence Titration Results. The fluorescence band of free DASPMI ($\lambda_{\text{exc}} \approx 440 \text{ nm}$) is obtained at 570 nm and on binding with ct-DNA strong increase in the fluorescence intensity of 570 nm band with a slight red shift could be observed which was inferred as weak minor groove binding.²²

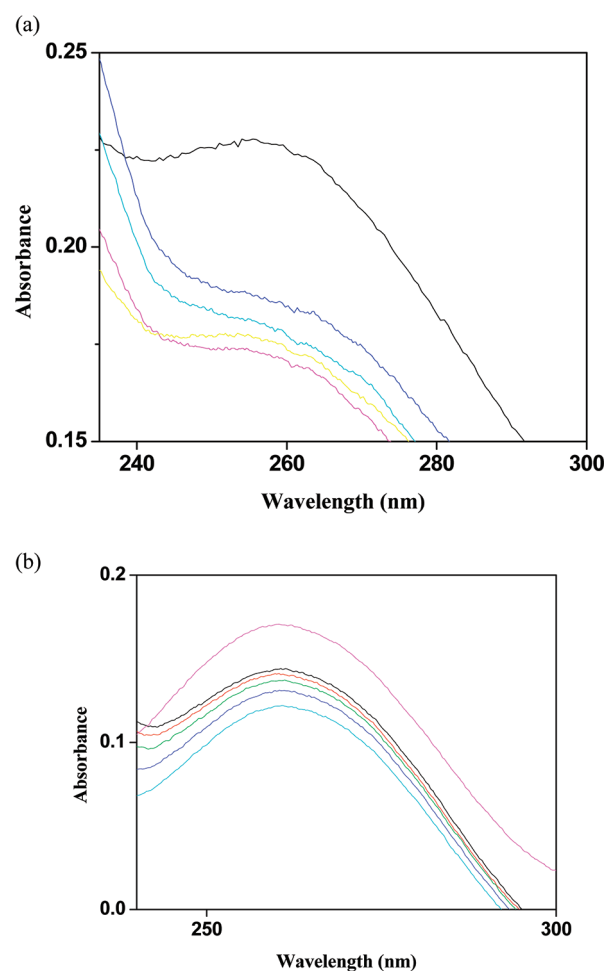


Figure 2. (a) Absorption spectra of ct-DNA (60 μM ; black line) with increasing concentration of vesicles and (b) absorbance spectra of ct-DNA (pink line), ct-DNA complexed with DASPMI (blue line), and ct-DNA complexed with DASPMI with addition of vesicles.

The intensity of 570 nm fluorescence band of free DASPMI increases with a slight blue shift ($\sim 8 \text{ nm}$) on gradual addition of the vesicles (Figure 3a). This blue shift of the DASPMI fluorescence band indicates the inclusion of the DASPMI molecules into the nonpolar interior of the vesicles. The TEM images of the vesicles with dark interior compared to the unloaded vesicles also confirm the inclusion of DASPMI in the vesicular interior³² as shown in Figure 3b. The inclusion of the DASPMI molecules into the vesicular core hinders the rotational motion of the DASPMI molecules around various bonds which consequently decreases the possible nonradiative process through the TICT state and thus the increase in DASPMI fluorescence intensity ensues.³³

In the buffer solution no tangible change in fluorescence intensity of NAPMD could be observed either in the case of neat NAPMD interacting with ct-DNA or the NAPMD attached to the vesicles interacting with ct-DNA. This suggests that both the neat NAPMD and NAPMD containing vesicle do not bind with ct-DNA, so we decided to encapsulate DASPMI by the vesicle to study the binding characteristics with ct-DNA. The fluorescence band intensity at 562 nm for DASPMI molecules loaded within the vesicle increases further along with a red shift of 3 nm with gradual addition of the ct-DNA (Figure 4), keeping the concentration of vesicles and DASPMI constant. Compared to DASPMI–ct-DNA interaction in buffer solution²²

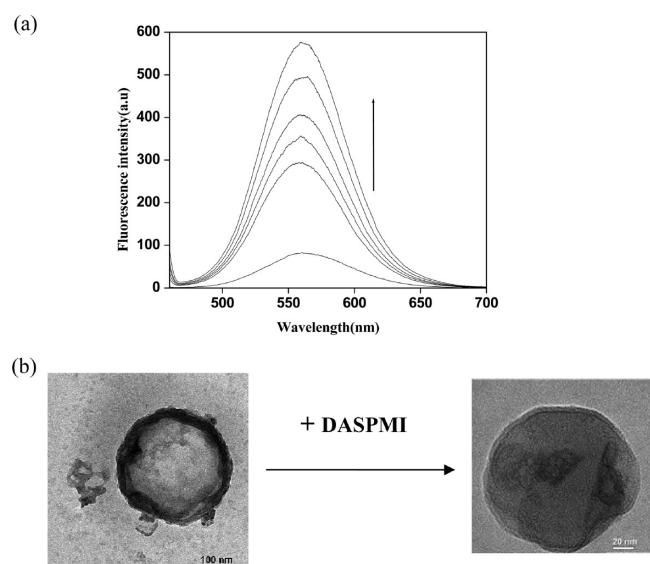


Figure 3. (a) Fluorescence spectra of DASPMI (0.05 mM) with gradual addition of vesicles. The arrow direction shows how the fluorescence of DASPMI responds to the increasing concentration of the vesicles. (b) TEM image of DASPMI encapsulated in the vesicles showing a dark interior as compared to the unloaded vesicles.

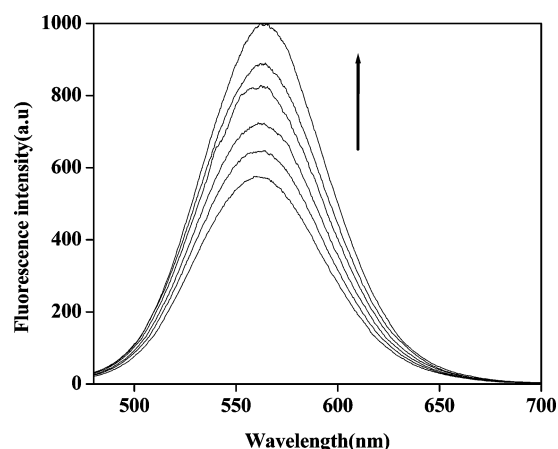


Figure 4. Fluorescence spectra of DASPMI (0.05 mM) in vesicle medium with increasing concentration of ct-DNA. The arrow direction shows how the fluorescence of DASPMI responds to the increasing concentration of the ct-DNA in vesicular medium. Ct-DNA concentration is increased as 0, 3, 6, 8, 12, 20, 40, and 60 μM .

with similar ct-DNA concentration the present increase in fluorescence intensity of DASPMI loaded inside vesicle is $\sim 150\%$. This increase in fluorescence intensity points to a further restriction of the rotational motion of DASPMI molecules around its various bonds. NAPMD molecules on vesicular wall interact with the DASPMI molecules in the core by energy transfer.²⁶ The effect of this energy transfer on DASPMI fluorescence while the addition of ct-DNA may be ruled out as in that condition no change in fluorescence intensity of NAPMD (excited at NAPMD absorption) or DASPMI fluorescence intensity could be observed.

3.3. SEM and TEM Results. If we look the SEM and TEM images vesicle interacting with DNA we observe a change in DNA structure. In SEM image free DNA shows clear distribution of DNA along with some aggregated forms (Figure 5a). The SEM image of the DNA with addition of vesicles loaded with

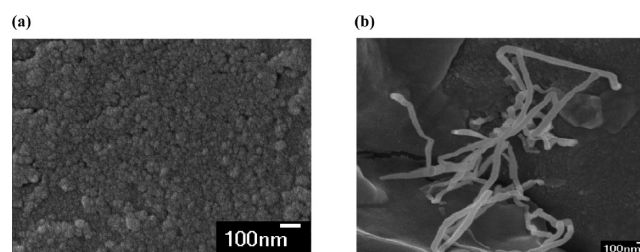


Figure 5. SEM image of (a) free ct-DNA (60 μM) in buffer solution and (b) ct-DNA added to the vesicle solution containing DASPMI.

DASPMI shows formation of some rod like structures (Figure 5b). These structures are similar to the rod shaped compaction structure of ct-DNA.^{34,35} It is already established that ct-DNA on compaction forms torroids or rods of about 100 nm dimension³⁶ and our results matches well with that.

To confirm this morphological transition of ct-DNA, we studied the TEM images (Figure 6) which are also very similar

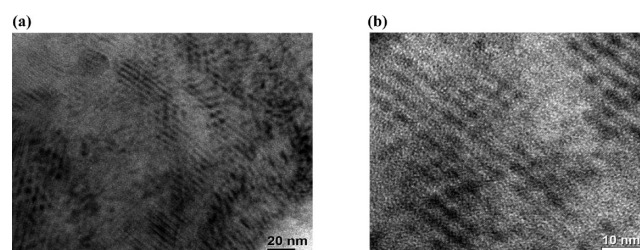


Figure 6. TEM image of ct-DNA (60 μM) condensate with the vesicles loaded with DASPMI molecules (a) in large scale and (b) in smaller scale.

to the compaction of ct-DNA by the vesicles as already been reported.³⁷ Now this ct-DNA compaction results in lamellar structures with definite packing regime and forms a hexagonal lattice.³⁶ In our case lattice structure could also be obtained in our TEM images as shown in Figure 7.

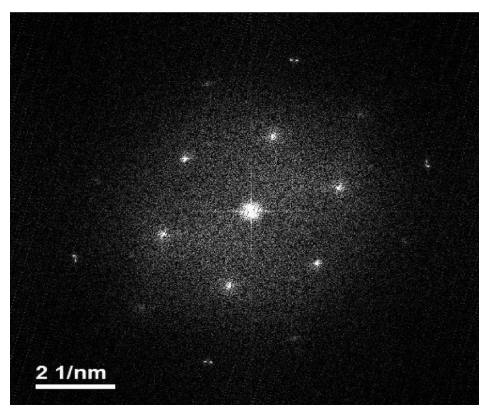


Figure 7. TEM image of hexagonal lattice packing of ct-DNA due to compaction by the vesicles.

3.4. Equilibrium Binding Titration. The binding constant (K) and the binding stoichiometry (n) for the complex formed by DASPMI molecules with ct-DNA in presence of the vesicles are determined from the fluorescence titration data. These spectral changes were used to estimate the binding constant for this binding mode of DASPMI to ct-DNA in presence of the vesicles.

The binding constant is evaluated using the following equation^{38,39}

$$\begin{aligned}\log[(F_0 - F)/F] &= \log K + n \log[\text{DNA}] \\ &= \log(\Delta F/F) \\ &= \log K + n \log[\text{DNA}]\end{aligned}\quad (1)$$

where F_0 and F are the fluorescence intensities of the fluorophore in absence and presence of different concentrations of ct-DNA in vesicular medium and K and n are binding constant and number of binding sites, respectively. A linear plot of $\log(\Delta F/F)$ vs $\log[\text{DNA}]$ is obtained (Figure 8) and the

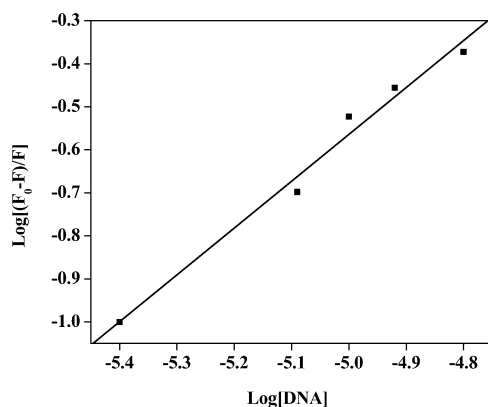


Figure 8. Plot of $\log(\Delta F/F)$ vs ct-DNA as determined from the fluorescence titration data.

Table 1. Equilibrium Binding Constant and Quenching Constant Values for DASPMI when Bound to ct-DNA in Different Media

system	n	K_b (M^{-1})	K_{sv} (M^{-1})
DASPMI + DNA in buffer solution	0.952	4.03×10^3	26.16
DASPMI + DNA in presence of	1.08	7.5×10^4	6

binding constant $K \approx 7.5 \times 10^4 M^{-1}$ and $n \approx 1.08$ (Table 1) could be obtained from the best fit of the plot. In our previous paper the binding constant was found to be $4.03 \times 10^3 M^{-1}$ and was assigned as minor groove binding of DASPMI with ct-DNA.²² Such a large increase (~ 20 times) of the binding constant value of DASPMI with ct-DNA in presence of the vesicles points toward strong binding of DASPMI with ct-DNA which is consistent with the other reported values of some typical intercalators.^{40–42} So this strongly points to intercalative binding of DASPMI with ct-DNA in vesicular medium.

3.5. Fluorescence Quenching Study. To confirm the type of binding mode of DASPMI with ct-DNA in vesicular medium, the fluorescence quenching of the DASPMI molecules was studied using KI as the ionic quencher. The fluorescence quenching studies give an idea about the availability of the probe molecules to the quencher and its steric bulk. Intercalative binding of the small molecules to the ct-DNA base pairs shields the molecules from the ionic quenchers, thus showing very low quenching compared to that in aqueous solution.⁴³ On the contrary, in the case of electrostatic and groove binding the molecules are exposed to the aqueous solution, thus making the molecule quite available to the ionic quenchers. So this quenching study can help us to get an insight

of the difference in DNA binding modes with DASPMI in presence and absence of the vesicles.

The fluorescence characteristics of free DASPMI, ct-DNA-DASPMI complex and ct-DNA-DASPMI complex in vesicular medium with gradual addition of KI were compared. The quenching phenomenon was studied using the Stern–Volmer equation

$$F_0/F = 1 + K_{sv}[Q] \quad (2)$$

The fluorescence bands for DASPMI in buffer solution and in ct-DNA environment get quenched with addition of KI. The quenching constants are obtained as $K_{sv} \approx 8.43$ and $26.16 M^{-1}$ in buffer solution and ct-DNA environment, respectively as reported in our previous paper.²² The fluorescence band for DASPMI in ct-DNA in vesicular medium also gets quenched with the addition of KI. The quenching constant is evaluated from the linear plot for the $F_0/F - 1$ vs $[Q]$ (Figure 9) and the

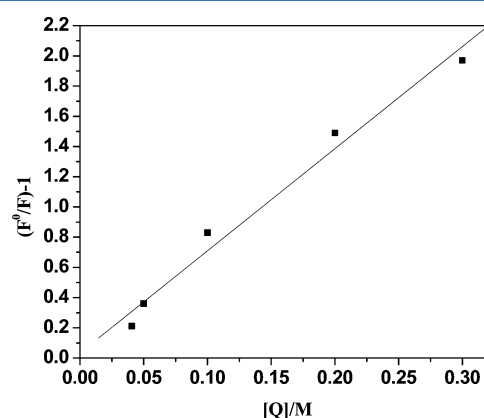


Figure 9. Stern–Volmer plot of DASPMI for quenching by KI.

value is obtained to be $K_{sv} \approx 6.7 M^{-1}$ which is much lower than that obtained in ct-DNA only (Table 1), indicating an intercalative binding.⁴² It seems that in vesicular medium the DASPMI molecules get stacked between the DNA base pairs which protect the molecules from the ionic quenchers.

3.6. CD Study. The morphology of DNA can be studied efficiently by CD spectroscopy during the dye-DNA interactions. The CD spectra of free ct-DNA (60 μM) shows a positive band at 273 nm due to base stacking and a negative band at 246 nm due to right handed helicity, this is a characteristics of the B-form of ct-DNA.^{44,45} These bands are highly sensitive toward the DNA interaction with small molecules.^{46,47} The changes in the CD spectra can be attributed to the corresponding changes in the ct-DNA structure.⁴⁸ The CD spectra shows almost no change in case of minor groove binding and electrostatic binding, whereas the intercalative binding affects both the positive and negative bands, as observed for classical intercalators, such as methylene blue.⁴⁹ Figure 10 shows the CD spectra of ct-DNA complexed with DASPMI in the vesicular medium. The figure shows that both the bands of the CD spectra are affected by the increasing concentration of the DNA to DASPMI in vesicular medium. This study shows that although DASPMI molecules are entrapped within the vesicles (Figure 3b), then also it interacts with the DNA and perturbs the DNA structure. In our earlier work²² the DASPMI was found not affecting the CD spectra of the ct-DNA thus showing minor groove binding. Figure 10b shows the CD spectra of ct-DNA

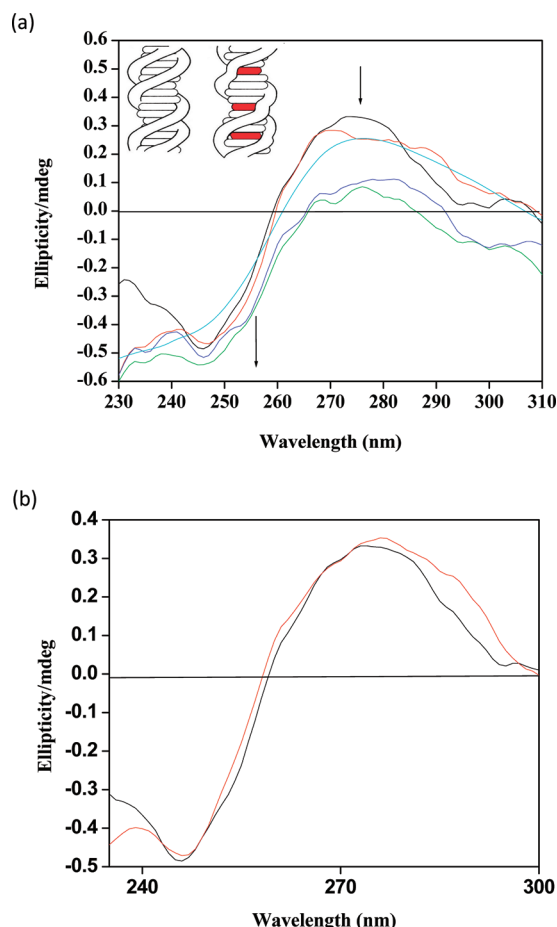


Figure 10. (a) Arrow showing the change in CD spectra of ct-DNA when complexes with DASPMI in the vesicular medium, with increasing concentration of DASPMI 0 M (black curve), 0.01 mM (red curve), 0.02 mM (blue curve), 0.04 mM (navy blue curve), and 0.05 mM (green curve). Inset-picture showing the distortion of the ct-DNA structure after intercalating with the DASPMI in vesicle medium. The red marks show the DASPMI molecules bounded intercalatively to the DNA, (b) CD spectra of DNA (60 μ M) (red line) and DNA with addition of vesicles (black line).

when interacted with vesicles both the positive and negative bands are affected. A red shift in the positive band is observed. It shows the vesicles alter the B-form of the DNA structure.⁵⁰

If we look at the absorbance titration (Figure 2) and CD results (Figure 10b) closely to obtain information at bulk level for the effect of vesicles only on DNA we find that the absorption band of DNA at 260 nm gets quenched, broadened and red-shifted by 3 nm. These spectral changes confirm that the vesicles interact with the base pairs⁵⁰ to perturb the electronic transition ($\pi\pi^*$) of DNA at 260 nm. The quenching of DNA absorbance peak with addition of vesicles shows increased level of DNA compaction with increasing concentration of vesicles. The CD spectra of free DNA (60 μ M) shows a positive band at 273 nm due to base stacking and a negative band at 246 nm due to right handed helicity, this is a characteristics of the B-form of ct-DNA. On addition of vesicles both the bands of ct-DNA get affected (Figure 5). The decrease in positive band shows possibility of destabilization of ct-DNA base stacking due to the interactions of vesicles with the ct-DNA base pairs.

In the case of retro-addition of the vesicles on the already bound ct-DNA with DASPMI molecules the 260 nm absorption band of DNA gets reduced with addition of DASPMI. On further addition of vesicles no relevant change is observed (Figure 2a) as compared to Figure 2b. This shows that vesicles have no effect on already bound ct-DNA with DASPMI⁵¹ (Scheme 1).

3.7. Fluorescence Lifetime Studies. The time constants for the biexponential decay of DASPMI in buffer solution are 0.6 ± 0.01 ns and 1.4 ± 0.01 ns for the LE (locally excited) state and the ICT state, respectively¹⁸ and inside the vesicle the decay time increases to 0.90 ± 0.01 ns and 2.02 ± 0.01 ns respectively. After interaction with ct-DNA the decay time of DASPMI in vesicular medium can also be fitted biexponentially with time constants 0.65 ± 0.01 and 2.40 ± 0.01 ns (Figure 11a), whereas the decay times for DASPMI interacting with ct-DNA in buffer solution are 0.65 ± 0.01 and 2.70 ± 0.01 ns. So the decay times are nearly the same for ct-DNA interacting with DASPMI in buffer solution or in vesicle medium. But an increase in lifetime of DASPMI in vesicles compared to that in buffer solution indicates that DASPMI binds with ct-DNA while in vesicular medium also.

Temporal fluorescence anisotropy decay was also determined to compare the DNA binding modes with DASPMI inside vesicle or outside. The fluorescence anisotropy decay time constant of DASPMI in ct-DNA increases to 0.15 and 5.20 ns (double component) compared to that in buffer solution (0.12 ns),²² which show a possible binding of DASPMI molecules to ct-DNA as obtained from our previous study. In the previous study²² the double component of decay time also predicted the presence of a wobbling motion of the dye when bound to ct-DNA. The anisotropy decay time constant of DASPMI in vesicle medium further slows down to 7.1 ns on interacting with ct-DNA (Figure 11b), giving a single component only (Table 2). Single component of anisotropy decay with increased decay time of the probe in vesicle medium points to the absence of wobbling motion of DASPMI²³ and much restricted motion of the dye within the ct-DNA, which is a strong point in favor of mode of binding of the probe with ct-DNA by intercalation. The initial anisotropy of DASPMI inside vesicular medium interacting with ct-DNA also increases to 0.4 compared to DASPMI-ct-DNA in buffer (0.36) (Table 2). This increase in anisotropy predicts much more confined medium around DASPMI bound with ct-DNA in vesicular medium compared to buffer solution. The anisotropy results also confirm that the presence of vesicles induce stronger binding of the DASPMI molecules to ct-DNA by intercalation rather than by weak minor groove binding.

In water solution DNA remains in elongated form due to the repulsion between the phosphate groups, on addition of a compaction agent DNA undergoes compaction. This compaction usually occurs due to the complexation with polycations. The electrostatic interactions reduce the monomer–monomer repulsion and causes collapse of DNA elongated structure.³⁶ The block-copolymers having PEG group can also cause the compaction of DNA by a process called psi-condensation.^{52,53} The compaction of DNA gives different shapes and sizes of the complexes it can be torroidal, globular or rod shaped.⁵⁴ On compaction some of the DNA strands mask the other DNA strands thus shielding the base pairs from the aqueous solution. This fact is also observed in KI quenching effect that in presence of vesicles the quenching rate of DASPMI by KI ($K_{sv} \approx 6.7$) is lower than even in aqueous solution ($K_{sv} \approx 8.43$). Due to the

Scheme 1. Pictorial Representation of the ct-DNA Binding Mode with DASPMI, from Groove to Intercalative, Induced by the Vesicles Also Showing No Change in the DNA Binding Mode for Already Bounded DASPMI Molecules to ct-DNA on Later Addition of the Vesicles

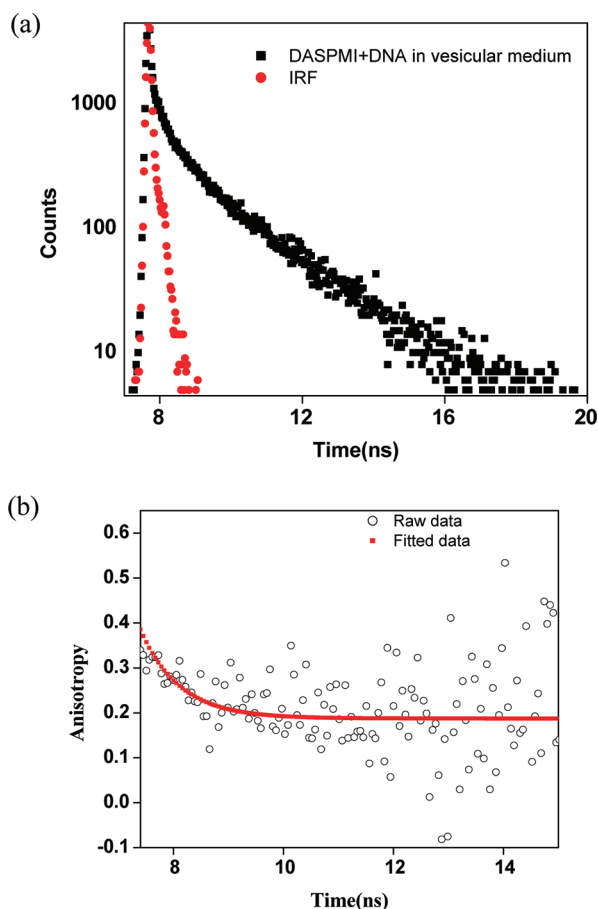
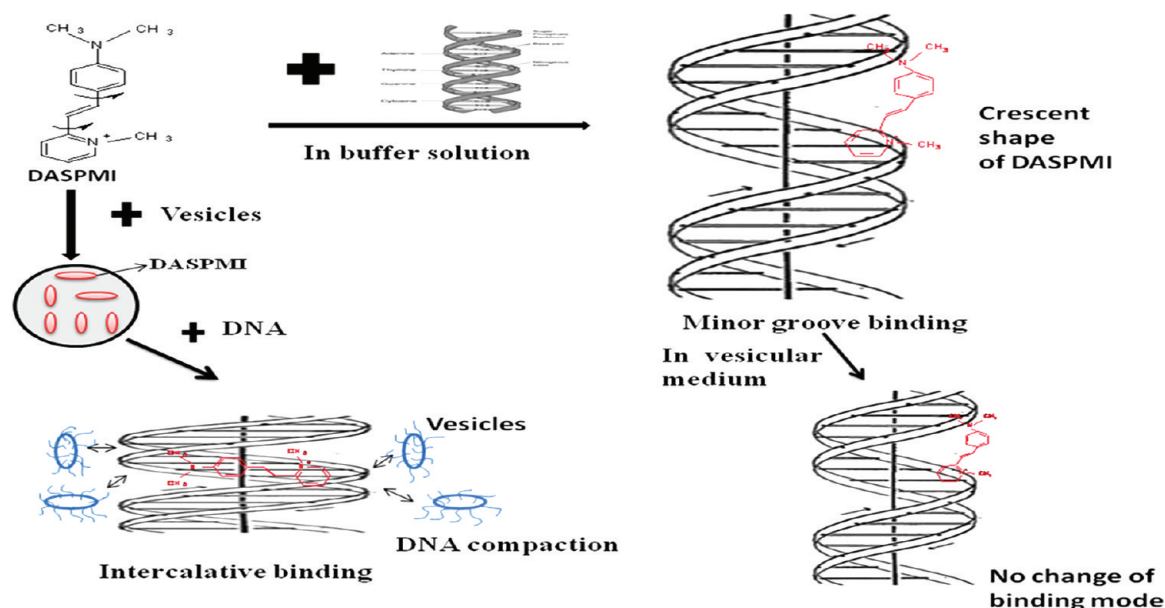


Figure 11. (a) Time resolved fluorescence decay rate of DASPMI in ct-DNA in vesicular medium. (b) Temporal anisotropy of DASPMI in ct-DNA in vesicular medium.

compaction of DNA the DASPMI molecules intercalate within the DNA base pairs which are partially masked from the

Table 2. Temporal Fluorescence Anisotropy Decay Data for DASPMI in Different Media

systems	τ_{a1} (ps)	a_1	τ_{a2} (ps)	a_2	r_0
buffer	120 ± 10	1			0.39
DASPMI + DNA in buffer	150 ± 10	0.59	5200 ± 20	0.41	0.36
DASPMI + DNA in presence of vesicles	7100 ± 10	1			0.4

aqueous solution which cause reduced quenching rate of DASPMI by KI than in aqueous solution. As was pointed before, the fluorescence results of DASPMI show that fluorescence band of DASPMI gets blue-shifted by 8 nm when inserted within the vesicles (Figure 3a). When DNA is added to the DASPMI molecules loaded within the vesicles a slight red shift of 3 nm is observed (Figure 4). This red shift shows that DASPMI partially gets out of the vesicles and interacts with the DNA. Since it does not come out fully to the aqueous solution rather it interacts with the DNA so instead of 8 nm shift we observe a smaller red shift of 3 nm. All of the above results prove the fact that addition of vesicles causes DNA compaction. The vesicles loaded with the DASPMI molecules interact directly with the DNA base pairs and in that process DASPMI comes out of vesicle partially and gets stacked between the DNA base pairs (Scheme 1).

4. CONCLUSION

In this work it has been shown that binding mode (groove) of the probe-ct-DNA in buffer solution can be changed in presence of vesicles. Normally DASPMI binds with ct-DNA by groove binding in buffer solution by attaining the crescent shape. The block-copolymer and anionic micelle are known to intercalate with each other to form nanocomposites. These nanocomposites interact with a charge transfer dye and form vesicles. DASPMI is observed to get encapsulated by these vesicles. The vesicles affect the base pairs to attain DNA compaction and in this condition of favorable electrostatic

condition and π - π interaction of NAPMD sitting on the vesicles and the base pairs the dye DASPMI gets partially out of the vesicles and stacked between the DNA base pairs by intercalative binding. However, the dye-DNA binding mode (minor groove) remains unchanged for retro-addition of the vesicles to the already groove bound dye molecules.

AUTHOR INFORMATION

Corresponding Author

*E-mail: spsc@iacs.res.in.

Notes

The authors declare no competing financial interest.

REFERENCES

- (1) Singh, M. P.; Joseph, T.; Kumar, S.; Bathini, Y.; Lown, J. W. *Chem. Res. Toxicol.* **1992**, *5*, 597–607.
- (2) Sparks, J.; Scholz, C. *Biomacromolecules*. **2009**, *10* (7), 1715–1719.
- (3) Lown, J. W. *Anti-Cancer Drug Des.* **1988**, *3*, 25–40.
- (4) Prento, P. *Biotech. Histochem.* **2001**, *76*, 137–161.
- (5) Lepecq, J. B.; Paoletti, C. *Anal. Biochem.* **1966**, *17*, 100–107.
- (6) Hill, B. T. *Anal. Biochem.* **1976**, *70*, 635–638.
- (7) Mouli Pandey, C.; Sumana, G.; Malhotra, B. D. *Biomacromolecules* **2011**, *12*, 2925–2932.
- (8) Ci, Y. X.; Li, Y. Z.; Liu, X. J. *Anal. Chem.* **1995**, *67*, 1785–1788.
- (9) Guo, X. Q.; Li, F.; Zhao, Y. B. *Anal. Lett.* **1998**, *31*, 991–1005.
- (10) Wahl, M.; Koberling, F.; Patting, M.; Rahn, E. H. *Curr. Pharm. Biotechnol.* **2004**, *5*, 299–308.
- (11) Haugland, R. G. *Handbook of Fluorescent Probes and Research Products*, 9th ed.; Molecular Probes Inc: Eugene, OR, 2002.
- (12) Barton, J. K. *J. Biomol. Struct. Dyn.* **1983**, *1*, 621–632.
- (13) Lerman, L. S. *J. Mol. Biol.* **1961**, *3*, 18–30.
- (14) Loew, L. M.; Bonneville, G. W.; Surow, J. *Biochemistry* **1978**, *17*, 4065–4071.
- (15) Loew, L. M.; Scully, S.; Simpson, L.; Waggoner, A. S. *Nature* **1979**, *281*, 497–499.
- (16) Loew, L. M.; Simpson, L. L. *Biophys. J.* **1981**, *34*, 353–365.
- (17) Bereiter-Hahn, J. *Biochim. Biophys. Acta* **1976**, *423*, 1–14.
- (18) Bereiter-Hahn, J.; Seipel, K. H.; Vöth, M.; Ploem, J. S. *Cell Biochem. Funct.* **1983**, *1*, 147–155.
- (19) Strehmel, B.; Seifert, H.; Rettig, W. J. *Phys. Chem. B* **1997**, *101*, 2232–2243.
- (20) Strehmel, B.; Rettig, W. J. *Biomed. Opt.* **1996**, *1*, 98–109.
- (21) Valeur, B. *Molecular Fluorescence: Principles and Applications*; Wiley-VCH: Weinheim, 2002.
- (22) Sahoo, D.; Bhattacharya, P.; Chakravorti, S. J. *Phys. Chem. B* **2010**, *114*, 2044–2050.
- (23) Srinivas, G.; Discher, D. E.; Klein, M. L. *Nat. Mater.* **2004**, *3*, 638–644.
- (24) Sahoo, D.; Bhattacharya, P.; Chakravorti, S. J. *Phys. Chem. B* **2009**, *113* (41), 13560–13565.
- (25) Manna, A.; Chakravorti, S. *Photochem. Photobiol.* **2012**, *88*, 285–294.
- (26) Manna, A.; Sahoo, D.; Chakravorti, S. J. *Phys. Chem. B* **2012**, *116*, 2464–2471.
- (27) (a) Long, E. C.; Barton, J. K. *Acc. Chem. Res.* **1990**, *23*, 271.
(b) Li, Q. G.; Wang, H. M.; Li, A. Z. *Molecular Biophysical Chemistry (Chinese)*; Higher Education Publisher: Beijing, 1992; p 276.
- (28) Korobko, A. V.; Backendorf, C.; van der Maarel, J. R. C. J. *Phys. Chem. B* **2006**, *110*, 14550–14556 and the references cited therein.
- (29) Gaballah, S. T.; Collier, G.; Netzel, T. L. *J. Phys. Chem. B* **2005**, *109*, 12175–12181.
- (30) Summers, D. P.; Noveron, J.; Basa, R. C. *Orig. Life Evol. Biosph.* **2009**, *39* (2), 127–140.
- (31) Cao, Y.; He, X. W. *Spectrochem. Acta Part A* **1998**, *54*, 883–892.
- (32) Zhang, X.; Rehm, S.; Safont-Sempere, M. M.; Wurthner, F. *Nature* **2009**, *1*, 623–629.
- (33) Ramdass, R.; Hahn, J. B. *J. Phys. Chem. B* **2007**, *111*, 7681–7690.
- (34) Maier, B.; Rädler, J. *Phys. Rev. Lett.* **1999**, *82*, 1911–1914.
- (35) Fang, Y.; Hoh, J. H. *FEBS Lett.* **1999**, *459*, 173–176.
- (36) *DNA Interactions with Polymers and Surfactants*; Dias, R., Lindman, B., Eds.; John Wiley & Sons, Inc.: Hoboken, NJ, 2008; p 75.
- (37) Estévez-Torres, A.; Baigl, D. *Soft Matter*. **2011**, *7*, 6746–6756.
- (38) Feng, X. Z.; Lin, Z.; Yang, L. J.; Wang, C.; Bai, C. L. *Talanta*. **1998**, *47*, 1223–1229.
- (39) Barik, A.; Priyadarsini, K. I.; Mohan, H. *Photochem. Photobiol.* **2003**, *77*, 597–603.
- (40) Brun, A. M.; Harriman, A. *J. Am. Chem. Soc.* **1992**, *114*, 3656–3660.
- (41) Asakawa, M.; Endo, K.; Tol, H.; Aoyama, Y. *Bull. Chem. Soc. Jpn.* **1992**, *65*, 2050–2055.
- (42) Kumar, C. V.; Asuncion, E. H. *J. Am. Chem. Soc.* **1993**, *115*, 8574–8553.
- (43) Kumar, C. V.; Asuncion, E. H. *Chem. Commun.* **1992**, *6*, 470–472.
- (44) Novakova, O.; Chen, H.; Vrana, O.; Rodger, A.; Sadler, P. J.; Brabec, V. *Biochemistry*. **2003**, *42*, 11544–11554.
- (45) Curtis-Johnson, W. In *CD of Nucleic Acids in Circular Dichroism, Principles and Applications*; Nakanishi, K., Berova, N., Woody, R. W., Eds.; VHS: New York, 1994; pp 523–540.
- (46) Uma Maheswari, P.; Palaniandavar, M. *J. Inorg. Biochem.* **2004**, *98*, 219–230.
- (47) Ivanov, V. I.; Minchenkova, L. E.; Schyolkina, A. K.; Poletayev, A. I. *Biopolymers* **1973**, *12*, 89–110.
- (48) Lincoln, P.; Tuite, E.; Norden, B. J. *Am. Chem. Soc.* **1997**, *119*, 1454–1455.
- (49) Norden, B.; Tjerneld, F. *Biopolymers* **1982**, *21*, 1713–1734.
- (50) Banerjee, T.; Dubey, P.; Mukhopadhyay, R. *Biochimie* **2010**, *92*, 846–851.
- (51) Sarkar, R.; Pal, S. K. *Biomacromolecules* **2007**, *8*, 3332–3339.
- (52) Yamasaki, Y.; Katayose, S.; Kataoka, K.; Yoshikawa, K. *Macromolecules* **2003**, *36*, 6276–6279.
- (53) *DNA Interactions with Polymers and Surfactants*; Dias, R., Lindman, B., Eds.; John Wiley & Sons, Inc.: Hoboken, NJ, 2008; p 81.
- (54) Arscott, P. G.; Li, A. Z.; Bloomfield, V. A. *Biopolymers* **1990**, *30*, 619–630.